DFT Study of the 1-Octene Metathesis Reaction Mechanism with WCl_6/C Catalytic System

Dilek Yüksel, Bülent Düz, and Fatma Sevin*

Department of Chemistry, Hacettepe University, Ankara 06800, Turkey

Received: July 30, 2007; Revised Manuscript Received: February 9, 2008

A catalytic system consisting of tungsten carbene generated from WCl_6 and an atomic carbon is investigated theoretically for the metathesis of 1-octene at B3LYP/extended LANL2DZ level of DFT. The ground-state geometries and charge distributions of the structures belonging to the reaction mechanism are located. Energetics for the complete set of reactions, involving the formation of the tungsten carbene precatalyst, $Cl_4W{=}CCl_2$, the formation of tungsten methylidene and tungsten heptylidene with this precatalyst, and finally productive and degenerative metathesis steps with these alkylidene species are calculated in terms of total electronic energy and thermal energies. The free-energy (ΔG_{298}) surfaces of the structures involved in the related reactions are constructed. In addition, solvent effects on the single point energies of the structures are investigated for two different solvents, namely, cyclohexane and chloroform. The results indicate that the formation of the catalytically active heptylidene is energetically favored in comparison to the formation of methylidene, while the degenerative and productive metathesis steps are competitive. In the catalytic cycle, the formation of ethylene is exothermic, while the formation of 7-tetradecene is endothermic. As expected, solvent effects on the metathesis reactions are minor and solvation does not cause any change in the directions of the overall metathesis reactions.

1. Introduction

Olefin metathesis is a powerful synthetic method, which has received increasing attention in the last few decades and is now considered one of the most important C−C double bond formation reactions in organic synthesis.[1–4] Utility of the reaction has triggered many investigations on catalyst systems for olefin metathesis reactions, and it has been found that these catalyst systems almost always contain a transition metal complex acting through formation of a metal carbene, which initiates and then propagates the reaction.[5]

After many attempts to explain the mechanism of catalysis by metal carbenes, the Hérisson−Chauvin metallocyclobutane mechanism[6] is greatly accepted. As seen in Scheme 1, the mechanism involves a transition metal carbene, which forms a metallocyclobutane with the olefin by a formal (2 + 2) cycloaddition and then with a (2 + 2) cycloreversion and dissociation leads to a new metal carbene and the olefin product. Although these basic steps of metathesis are well-known and confirmed with many studies by now, a detailed mechanism of olefin metathesis by metal carbene complexes has been the subject of intense experimental and computational studies. Computations have contributed a lot in clarifying the mechanism especially with respect to the structure of the involved intermediates.[7] There have been a number of recent studies, both experimentally[8–19] and computationally,[20–46] in an attempt to clarify the olefin metathesis with metal carbenes. In many of these studies, model substrates are used to mainly reduce the computing cost, but it is important to note that only the real full-DFT system is able to reproduce the experimental results. Besides modest changes in the bond distances going from the model system to the real system, notably the conformation of the ligands changes.[7]

SCHEME 1: Hérisson−Chauvin Metallocyclobutane Mechanism

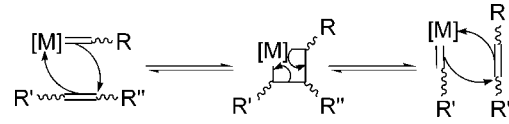

In the current study, DFT calculations at B3LYP/extended LANL2DZ level are employed to 1-octene within the WCl_6/C catalytic system to gain more realistic results. According to our former experimental work, it has been found that, in the metathesis of 1-octene with in situ WCl_6/ carbon atom catalytic system, the active species that initiates the metathesis was the tungsten carbene, $[W]{=}CCl_2$.[47] Now, we present the reaction energetics of metathesis steps of 1-octene with the precatalyst, $Cl_4W{=}CCl_2$, in terms of electronic and thermal energy values. Geometries of all structures in the relevant reaction paths, charge distribution on these structures, and gas phase single point energies in comparison with the single point energies in the presence of two different solvents, cyclohexane and chloroform, are also given.

2. Computational Details

The quantum chemical calculations are carried out by density functional theory (DFT),[48–52] since it usually gives realistic geometries, relative energies, and vibrational frequencies for transition metal compounds.[25–28] All calculations presented in this work are performed with the Gaussian 03, revision B.03 molecular modeling program.[53] All geometries are fully optimized without any symmetry restrictions by using Becke three-term functional with Lee−Yang−Parr exchange correlation (B3LYP)[54,55] in combination with the Los Alamos National Laboratory 2-double-zeta, (LANL2DZ)[56] basis set, adding extra d functions for Cl and C atoms and a p function to H atom to improve the geometries.[57] This basis set is denoted here as

* Corresponding author. E-mail: sevin@hacettepe.edu.tr. Telephone: +90 312 2977959. Fax: +90 312 2992163.

10.1021/jp076044c CCC: $40.75
Published on Web 04/29/2008

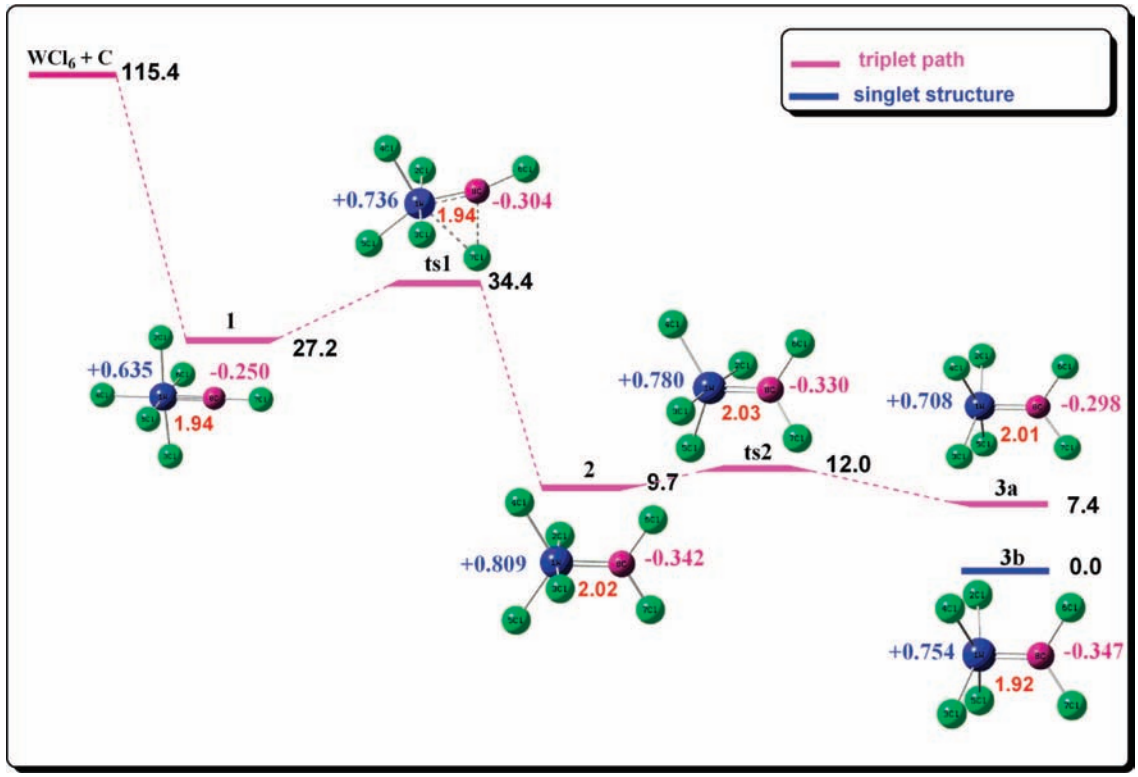

Figure 1. ΔG_{298} (kcal/mol) profile, W−C bond lengths (Å, red) and Mulliken charges (blue for W and magenta for C) in the WCl_6/ C system.

TABLE 1: Energetics for the Formation of Tungsten Carbenes in WCl_6/C System Calculated at B3LYP/Extended LANL2DZ Level

transition	ΔE (kcal/mol)	$\Delta E^{\ddagger}$ (kcal/mol)	ΔG_{298} (kcal/mol)	$\Delta G^{\ddagger}_{298}$ (kcal/mol)	ΔH (kcal/mol)	$\Delta H^{\ddagger}$ (kcal/mol)	ΔS (cal/mol K)	$\Delta S^{\ddagger}$ (cal/mol K)
$WCl_6 + C \rightarrow$ **1**	−92.0		−88.2		−92.6		−14.7	
1 → **ts1**		5.9		7.2		5.5		−5.6
1 → **2**	−18.1		−17.5		−18.2		−2.3	
2 → **ts2**		1.1		2.3		0.5		−6.0
2 → **3a**	−1.9		−2.3		−2.0		1.1	
3a → **3b**	−8.7		−7.4		−8.8		−4.7	

TABLE 2: Energetics for the Initiation Step of Catalytic Metathesis of 1-Octene with Tungsten Carbene, 3b, Calculated at B3LYP/Extended LANL2DZ Level

transition	ΔE (kcal/mol)	$\Delta E^{\ddagger}$ (kcal/mol)	ΔG_{298} (kcal/mol)	$\Delta G^{\ddagger}_{298}$ (kcal/mol)	ΔH (kcal/mol)	$\Delta H^{\ddagger}$ (kcal/mol)	ΔS (cal/mol K)	$\Delta S^{\ddagger}$ (cal/mol K)
3b + C_8 → **ts3a**		19.4		34.4		18.6		−52.9
3b + C_8 → **ts3b**		18.4		34.0		17.4		−55.4
3b + C_8 → **4a**	−2.5		13.1		−3.2		−54.7	
3b + C_8 → **4b**	−1.7		13.5		−2.4		−53.2	
4a → **ts4a**		20.8		20.0		20.8		2.5
4b → **ts4b**		25.3		25.2		24.7		0.4
4a → **5** + **6**	−7.1		−22.1		−6.5		52.3	
4b → **7** + **8**	−3.7		−18.9		−3.1		53.3	

extended LANL2DZ. The stability of the wave functions is confirmed with stability tests. The optimized geometries are also subjected to full frequency analyses at the same level of theory to verify the nature of the stationary points. Equilibrium geometries are characterized by the absence of imaginary frequencies, whereas the transition state geometries exhibit only one imaginary frequency in the reaction coordinate. For transition state (TS) geometries, confirmation calculations, involving intrinsic reaction coordinates (IRC) calculations, are performed in which the path connecting reagents, TS, and products are mapped. The energy values that are given in the results are the total electronic energies, enthalpies, and Gibbs free-energies at 298 K for an isolated system in the gas phase, so both the electronic and the thermal effects are considered in this study. Charge distribution on the atoms of the structures is presented in terms of the Mulliken charge,[58] which is based on orbital occupancies. Solvent effects on the single point energies of the structures are investigated via self-consistent reaction field calculations carried out for metathesis reactions in cyclohexane (dielectric constant 2.0) and in chloroform (dielectric constant 4.9) using the gas phase optimized geometries and a polarizable continuum model (PCM)[59] at the B3LYP/LANL2DZ level.

3. Results and Discussion

Reaction energetics of the catalytic metathesis of 1-octene with the WCl_6/C catalytic system is investigated computa-

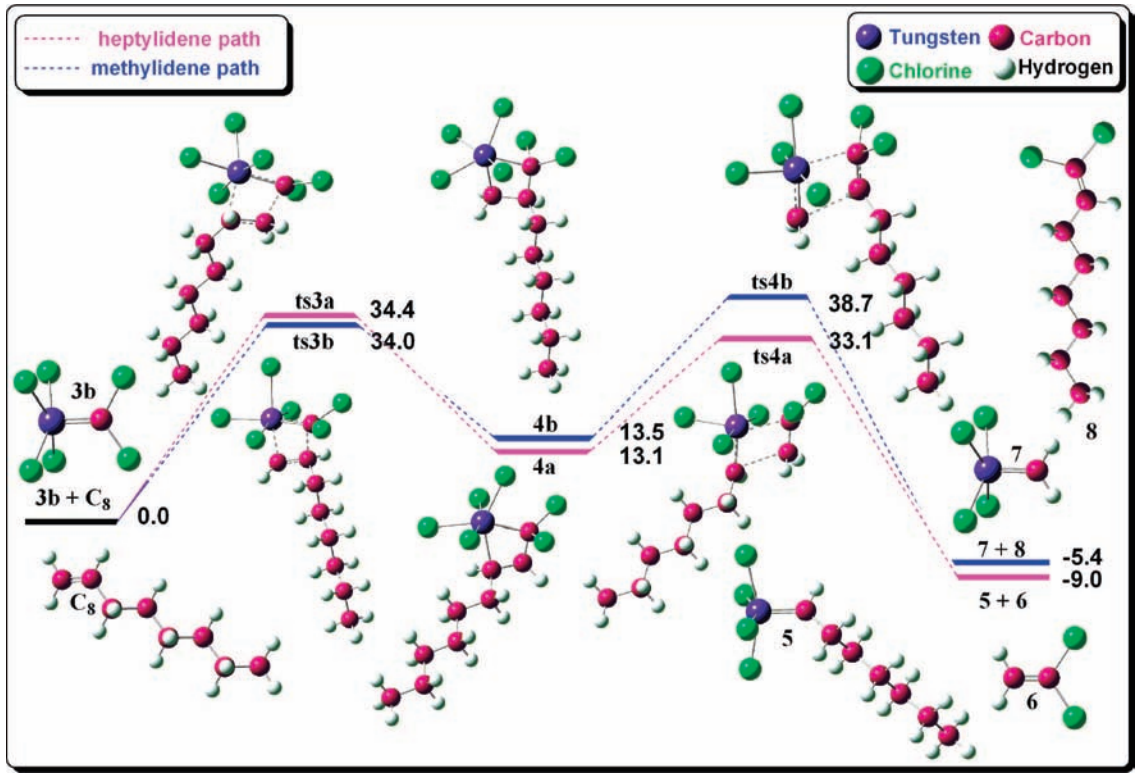

Figure 2. ΔG_{298} (kcal/mol) profile for the formation of initiation step of catalytic metathesis of 1-octene with tungsten carbene, **3b**.

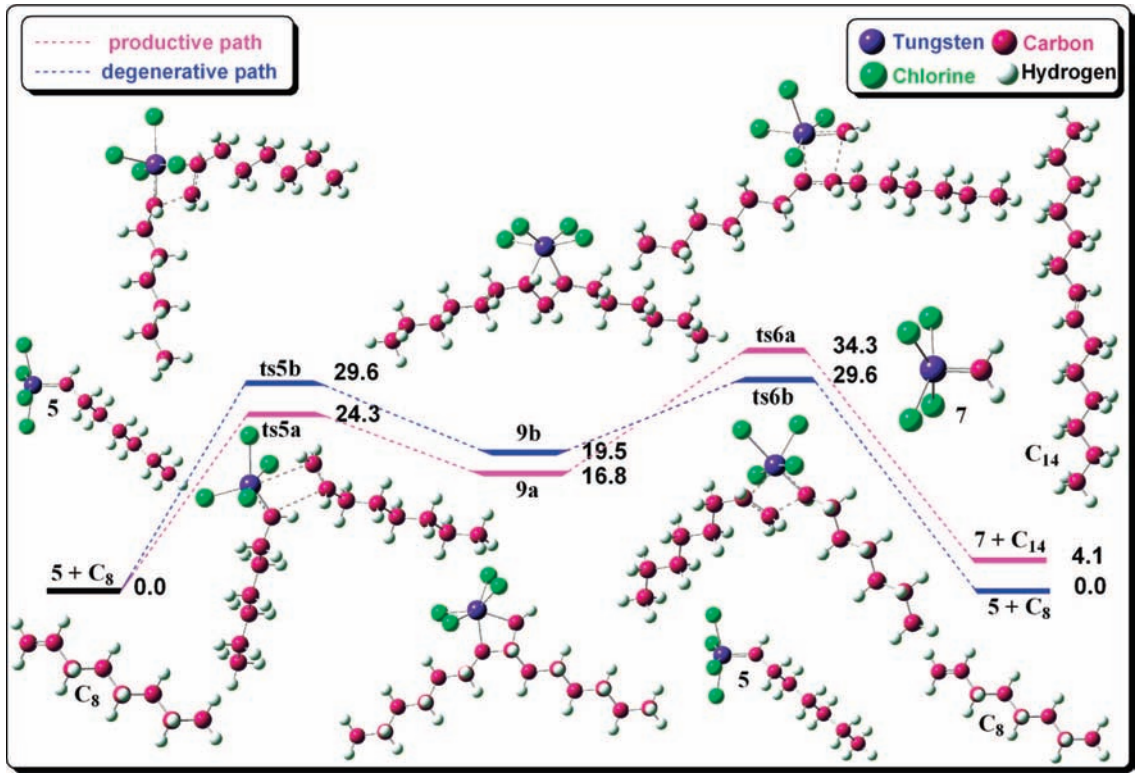

Figure 3. ΔG_{298} (kcal/mol) profile for the productive and the degenerative metathesis of 1-octene with tungsten heptylidene, **5**.

tionally in three steps. The first step is the formation of $Cl_4W{=}CCl_2$ precatalyst from WCl_6 and a C atom (Figure 1, Table 1). This step of the mechanism was previously published[47] without thermal energy values, which are included now. The second step is the conversion of this precatalyst to metathetically active methylidene and heptylidene species via the reaction with 1-octene (Figure 2, Table 2), and the third step contains productive and degenerative metathesis reactions of these alkylidenes with 1-octene (Figures 3 and 4, Tables 3 and 4). Table 5 shows the calculated bond lengths and bond angles of the metallocyclobutane intermediates involved in the metathesis steps (See also Supporting Information for detailed structural data and LANL2DZ geometries). The mechanistic model is mainly based on the metal carbene−metallocyclobutane mechanism proposed by Chauvin and Hérisson.[6]

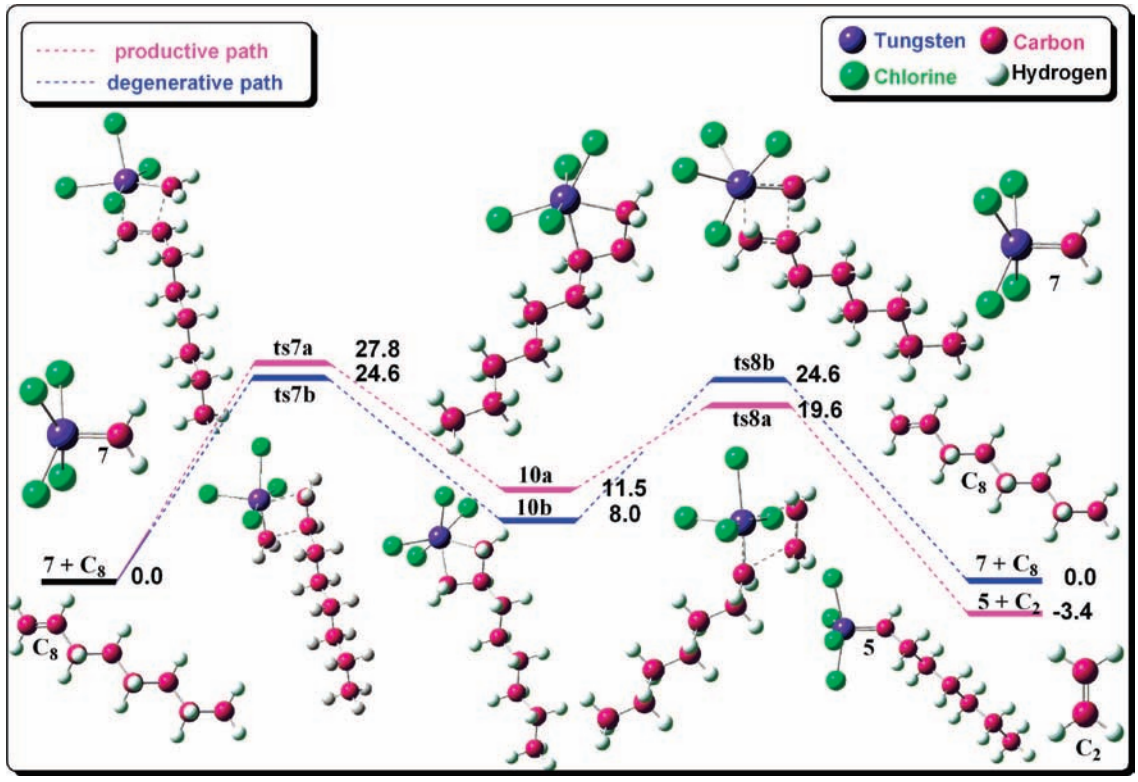

Figure 4. ΔG_{298} (kcal/mol) profile for the productive and the degenerative metathesis of 1-octene with tungsten methylidene, **7**.

TABLE 3: Energetics for the Productive and the Degenerative Metathesis of 1-Octene with Tungsten Heptylidene, 5, Calculated at B3LYP/Extended LANL2DZ Level

transition	ΔE (kcal/mol)	$\Delta E^{\ddagger}$ (kcal/mol)	ΔG_{298} (kcal/mol)	$\Delta G^{\ddagger}_{298}$ (kcal/mol)	ΔH (kcal/mol)	$\Delta H^{\ddagger}$ (kcal/mol)	ΔS (cal/mol K)	$\Delta S^{\ddagger}$ (cal/mol K)
5 + C_8 → **ts5a**		11.6		24.3		11.6		−42.8
5 + C_8 → **ts5b**		15.0		29.6		14.3		−51.3
5 + C_8 → **9a**	1.8		16.8		1.0		−53.0	
5 + C_8 → **9b**	4.7		19.5		3.9		−52.0	
9a → **ts6a**		18.1		17.5		18.3		2.6
9b → **ts6b**		10.4		10.1		10.4		0.7
9a → **7** + C_{14}	2.8		−12.7		3.7		54.8	
9b → **5** + C_8	−4.7		−19.5		−3.9		52.0	

TABLE 4: Energetics for the Productive and the Degenerative Metathesis of 1-Octene with Tungsten Methylidene, 7, Calculated at B3LYP/Extended LANL2DZ Level

transition	ΔE (kcal/mol)	$\Delta E^{\ddagger}$ (kcal/mol)	ΔG_{298} (kcal/mol)	$\Delta G^{\ddagger}_{298}$ (kcal/mol)	ΔH (kcal/mol)	$\Delta H^{\ddagger}$ (kcal/mol)	ΔS (cal/mol K)	$\Delta S^{\ddagger}$ (cal/mol K)
7 + C_8 → **ts7a**		13.4		27.8		12.5		−51.4
7 + C_8 → **ts7b**		10.2		24.6		9.2		−51.7
7 + C_8 → **10a**	−2.8		11.5		−3.6		−50.4	
7 + C_8 → **10b**	−5.9		8.0		−6.7		−49.3	
10a → **ts8a**		8.0		8.1		7.9		−0.8
10b → **ts8b**		16.0		16.6		15.9		−2.4
10a → **5** + C_2	−1.9		−14.9		−0.7		47.7	
10b → **7** + C_8	5.9		−8.0		6.7		49.3	

3.1. Formation and Structure of the Tungsten Carbene Precatalyst. All possible structures existing on the potential energy surface of the WCl_6/C system are constructed both at triplet and singlet spin states. Relative free-energies (kilocalories per mole, black), W−C bond lengths (Å, red), and the Mulliken charges on W (blue) and C (magenta) atoms are given in Figure 1.

In the triplet state, structure **1** is the first-formed structure from WCl_6 and atomic carbon with a formation free-energy, −88.2 kcal/mol. In the structure **1**, atomic carbon and the tungsten metal center of WCl_6 form a 1.94 Å W−C bond via insertion of atomic carbon into one of the W−Cl single bonds. This structure is then converted into the structure, **2**, through a transition state, **ts1**, with an activation free-energy, 7.2 kcal/mol. During this course, the charge on the tungsten atom increases gradually from 0.487 (**WCl_6**) to 0.809 (**2**) and a 2.02 Å W−C bond is formed, which is a double bond within experimental results.[60,61] Finally, with a geometric isomerization, **2** becomes the most stable triplet structure of the system, **3a**, through **ts2** with an activation free-energy, 2.3 kcal/mol. **3a** has a 2.01 Å W−C double bond, and the charges on W and C atoms are 0.708 and −0.298, respectively.

TABLE 5: Selected Bond Lengths (Angstroms) and Angles (Degrees) for Metallocyclobutane Intermediates[a]

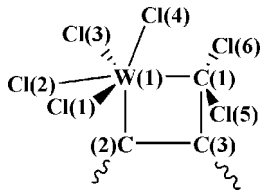

intermediate	bond	bond length (Å)	angle	angle (°)
4a	W(1)−Cl(1)	2.333	Cl(1)−W(1)−Cl(3)	162.9
	W(1)−Cl(2)	2.340	C(2)−W(1)−C(1)	62.6
	W(1)−C(1)	2.220	C(1)−C(3)−C(2)	98.0
	W(1)−C(2)	2.209		
	C(1)−C(3)	1.513		
	C(2)−C(3)	1.538		
4b	W(1)−Cl(1)	2.355	Cl(1)−W(1)−Cl(3)	158.6
	W(1)−Cl(2)	2.340	C(2)−W(1)−C(1)	61.6
	W(1)−C(1)	2.221	C(1)−C(3)−C(2)	95.1
	W(1)−C(2)	2.202		
	C(1)−C(3)	1.531		
	C(2)−C(3)	1.541		
9a	W(1)−Cl(1)	2.351	Cl(1)−W(1)−Cl(3)	146.5
	W(1)−Cl(2)	2.345	C(2)−W(1)−C(1)	62.4
	W(1)−C(1)	2.177	C(1)−C(3)−C(2)	96.0
	W(1)−C(2)	2.204		
	C(1)−C(3)	1.521		
	C(2)−C(3)	1.535		
9b	W(1)−Cl(1)	2.356	Cl(1)−W(1)−Cl(3)	161.4
	W(1)−Cl(2)	2.351	C(2)−W(1)−C(1)	63.6
	W(1)−C(1)	2.160	C(1)−C(3)−C(2)	96.9
	W(1)−C(2)	2.165		
	C(1)−C(3)	1.522		
	C(2)−C(3)	1.524		
10a	W(1)−Cl(1)	2.309	Cl(1)−W(1)−Cl(3)	167.8
	W(1)−Cl(2)	2.356	C(2)−W(1)−C(1)	62.4
	W(1)−C(1)	2.172	C(1)−C(3)−C(2)	97.7
	W(1)−C(2)	2.254		
	C(1)−C(3)	1.515		
	C(2)−C(3)	1.533		
10b	W(1)−Cl(1)	2.349	Cl(1)−W(1)−Cl(3)	147.6
	W(1)−Cl(2)	2.348	C(2)−W(1)−C(1)	62.1
	W(1)−C(1)	2.179	C(1)−C(3)−C(2)	94.6
	W(1)−C(2)	2.176		
	C(1)−C(3)	1.529		
	C(2)−C(3)	1.527		

[a] Geometric parameter optimized at B3LYP/extended LANL2DZ level.

In the singlet state, a stepwise mechanism leading to the formation of a tungsten carbene could not be constructed. All attempts give only one significant zero order stationary point corresponding to the structure, **3b**, which is very similar to **3a**. When these two structures are compared, it is seen that the geometries are similar, but the W−C bond distance is shorter (1.92 Å) and polarization of the W−C bond is higher for the singlet state. **3b** is 7.4 kcal/mol more stable than **3a** by means of free-energy. According to these calculations, it is assumed that the experimentally obtained[47] active carbene species, $[W]{=}CCl_2$, has a five coordinate square pyramidal geometry as in **3b**, which has a nucleophilic carbon atom with a partially negative charge (−0.347) bonded to the electrophilic metal center with a partially positive charge (+0.754). Besides the relative free-energies (ΔG_{298}), the relative enthalpy (ΔH), relative entropy (ΔS) and the relative total electronic energy (ΔE) values of the structures of this step are tabulated in Table 1. As expected, the formation of the carbene species from WCl_6 and atomic carbon lowers the entropy of the system, but since the carbon atom is highly energetic, it is seen that the formation of all of the tungsten carbene species are exothermic reactions.

3.2. Initiation Step of Metathesis. The different geometrical approaches of 1-octene, toward the precatalyst **3b**, lead to the formation of two types of catalytically active alkylidene species via two different reaction paths of relative free-energy designated with **a** and **b** notations in Figure 2.

In the heptylidene path, the coordination of 1-octene to the metal center of **3b** forms a metallocyclobutane ring, **4a**, through the activation complex **ts3a** with an activation free-energy 34.4 kcal/mol. The W−C double bond of **3b** (1.92 Å) increases to 2.11 Å in **ts3a**, and it becomes a single bond (2.22 Å) in **4a**. The charge on W decreases from 0.754 to 0.583 in **ts3a** and becomes 0.374 in **4a**. Afterward, the ring opens to form the tungsten heptylidene, **5**, and the structure **6** through a second transition state **ts4a** with an activation free-energy 20.0 kcal/mol. In **ts4a**, the W−C bond is about to be broken with a length 2.34 Å, as expected.

On the other hand, in the methylidene path, through a transition state **ts3b**, 1-octene and **3b** form another cylobutane ring, **4b**, with an activation free-energy 34.0 kcal/mol. This ring then opens to form the methylidene, **7**, and the structure **8** via **ts4b** with an activation free-energy 25.2 kcal/mol. In the structures **ts3b**, **4b**, and **ts4b**, the W−C bond lengths are 2.10, 2.22, and 2.40 Å, respectively. The charges on W in the mentioned structures are 0.482, 0.325, and 0.377, respectively.

Calculated transition energetics, in terms of total electronic energy, free-energy, enthalpy, and entropy, within the structures of the initiation step, are given in Table 2. Both methylidene ($\Delta H_f = -5.5$ kcal/mol) and heptylidene ($\Delta H_f = -9.7$ kcal/mol) formations are exothermic reactions with negative enthalpy values, but it is seen that the formation of heptylidene, **5**, is energetically more favorable than the formation of the methylidene species, **7**, in this step.

3.3. Productive and Degenerative Metathesis Steps. The heptylidene **5** and the methylidene **7** enter the same set of reactions with 1-octene as in the initiation step. Relative free-energy path of productive and degenerative metathesis reactions of 1-octene in the presence of the heptylidene, **5**, is given in Figure 3, and that of methylidene, **7**, is given in Figure 4.

Again, relative to the geometrical approach of 1-octene, $\mathbf{C_8}$, toward the tungsten carbene **5**, metallocyclobutane intermediates **9a** and **9b** are formed through the transition states **ts5a** and **ts5b** with activation free-energies 24.3 and 29.6 kcal/mol, respectively. The metallocyclobutane **9a** produces the metathesis product 7-tetradecene, $\mathbf{C_{14}}$, through **ts6a** with an activation free-energy 17.5 kcal/mol, while **9b** degenerates to the starting structures, **5** and $\mathbf{C_8}$, through **ts6b** with an activation free-energy 10.1 kcal/mol.

The values of W−C bond lengths in the structures **ts5a**, **9a**, and **ts6a**, are 1.91, 2.20, and 2.35 Å, while the charge on W in the corresponding structures are 0.557, 0.322, and 0.236, respectively. In the degenerative path, the structures **ts5b**, **9b**, and **ts6b** have the W−C bond lengths 2.00, 2.16, and 2.00 Å, and the charges on W in these structures are 0.466, 0.351, and 0.466, respectively. All of these values are in the expected range for the broken and formed bonds in the process.

The metathesis of 1-octene with methylidene, **7**, forms ethylene, $\mathbf{C_2}$, as a metathesis product via similar reactions. The metallocyclobutane intermediates **10a** and **10b** are formed through the transition states **ts7a** and **ts7b** with activation free-energies 27.8 and 24.6 kcal/mol, respectively. The metallocyclobutane **10a** produces the metathesis product ethylene, $\mathbf{C_2}$,

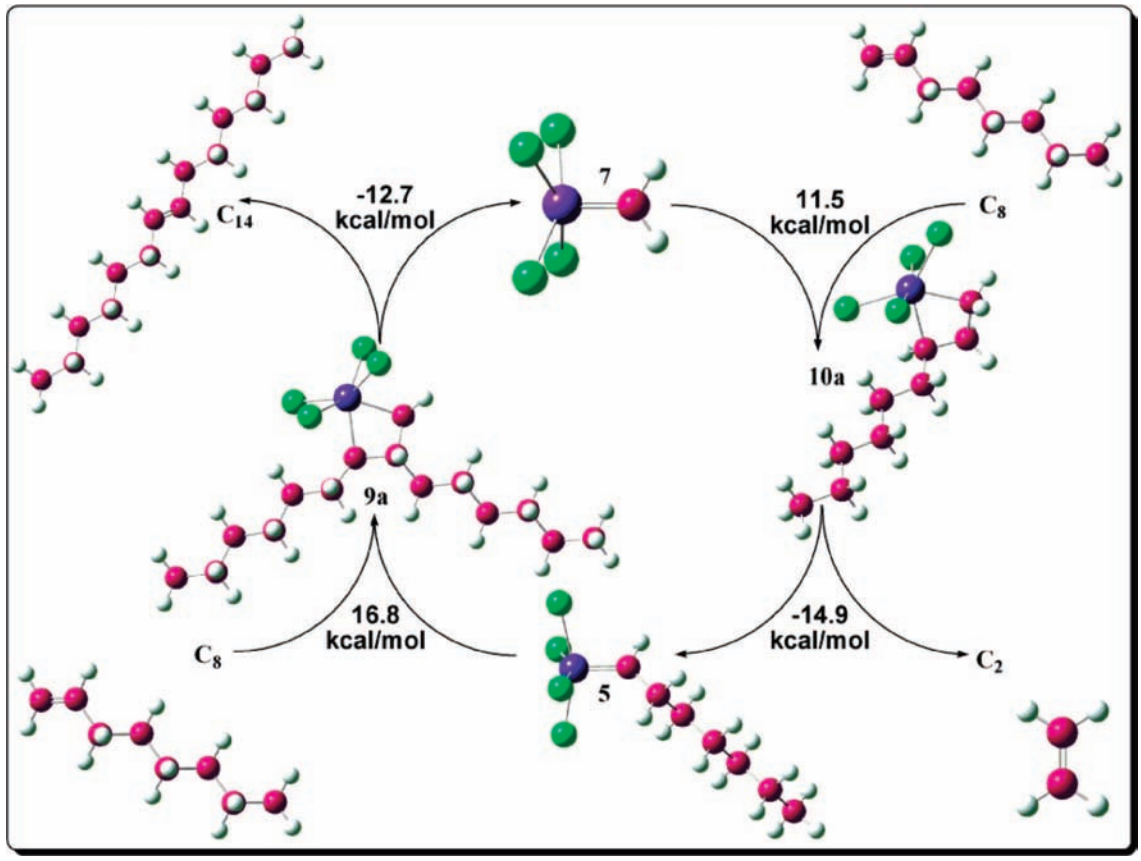

Figure 5. ΔG_{298} (kilocalories per mole) profile for the Chauvin mechanism for metathesis of 1-octene with tungsten alkylidenes, **5** and **7**.

through **ts8a** with an activation free-energy 8.1 kcal/mol, while **10b** degenerates to the starting structures, **7** and $\mathbf{C_8}$, through **ts8b** with an activation free-energy 16.6 kcal/mol.

In the structures **ts7a**, **10a**, and **ts8a**, the W−C bond lengths are 1.97, 2.17, and 2.19 Å, respectively. The charges on W in the related structures are 0.357, 0.325, and 0.436, respectively. In the structures **ts7b**, **10b**, and **ts8b**, the W−C bond lengths are 1.97, 2.18, and 1.97 Å, respectively. The charges on W in these structures are 0.341, 0.282, and 0.341, respectively. As can be seen in Table 3 and Table 4, enthalpy effects precede the effect of entropy, and formation of 7-tetradecene is an endothermic process ($\Delta H_f = 4.7$ kcal/mol), while the formation of ethylene is exothermic ($\Delta H_f = -4.3$ kcal/mol).

3.4. Metathetic Cycle. The productive metathesis reactions given in Figures 3 and 4 are summarized with a catalytic cycle seen in Figure 5. Within the catalytic cycle, the heptylidene, **5**, is converted to the methylidene, **7**, with a free-energy of reaction, $\Delta G_{298} = 4.1$ kcal/mol, which is in turn converted back to the heptylidene, **5**, with a free-energy of reaction $\Delta G_{298} = -3.4$ kcal/mol. During the conversion of **5** to **7**, the metathesis product 7-tetradecene, $\mathbf{C_{14}}$, is formed, while ethylene, $\mathbf{C_2}$, is formed when **5** is converted to **7**. The overall process is endothermic ($\Delta H = 0.4$ kcal/mol; see Table 3 and Table 4) and favored to the formation of ethylene with $\Delta G_{298} = 0.7$ kcal/mol, as far as the free-energy values are concerned.

3.5. Solvent Effects on Energies of the Reaction Paths. Table 6 shows the differences in single point energies between gas phase and solutions of cyclohexane and chloroform for the metathesis of 1-octene ($\mathbf{C_8}$) with **3b**. These differences are more evident for chloroform, when compared with cyclohexane. When the activation steps are investigated, it is seen that solvation causes mostly a decrease in activation energies of transition states. Main decreases in activation energies due to solvation are seen in the transition states, **ts4a**, **ts4b**, and **ts8a**, which are 4.8, 4.0, and 5.0 kcal/mol by chloroform and 2.4, 2.0, and 2.6

TABLE 6: Solvent Effects on the Energetics of the Metathesis Reactions (Kilocalories per Mole)

	gas phase		cyclohexane		chloroform	
reaction	ΔE^a	$\Delta E^{\ddagger b}$	ΔE^a	$\Delta E^{\ddagger b}$	ΔE^a	$\Delta E^{\ddagger b}$
STEP 2						
3b + $\mathbf{C_8}$ → **ts3a**		14.9		14.8		15.6
3b + $\mathbf{C_8}$ → **ts3b**		12.6		12.6		13.6
3b + $\mathbf{C_8}$ → **4a**	−7.6		−7.2		−5.9	
3b + $\mathbf{C_8}$ → **4b**	−7.9		−7.3		−5.9	
4a → **ts4a**		18.6		16.2		13.8
4b → **ts4b**		23.9		21.9		19.9
4a → **5** + **6**	−5.5		−7.6		−10.2	
4b → **7** + **8**	−0.8		−2.9		−4.9	
STEP 3						
5 + $\mathbf{C_8}$ → **ts5a**		11.0		12.2		14.0
5 + $\mathbf{C_8}$ → **ts5b**		13.1		13.0		12.8
5 + $\mathbf{C_8}$ → **9a**	3.0		4.4		6.1	
5 + $\mathbf{C_8}$ → **9b**	6.5		7.9		9.8	
9a → **ts6a**		14.6		13.1		12.0
9b → **ts6b**		6.6		5.2		3.1
9a → **7** + $\mathbf{C_{14}}$	2.9		1.8		0.5	
9b → **5** + $\mathbf{C_8}$	−6.5		−7.9		−9.8	
STEP 4						
7 + $\mathbf{C_8}$ → **ts7a**		9.0		9.2		9.8
7 + $\mathbf{C_8}$ → **ts7b**		10.9		10.4		10.1
7 + $\mathbf{C_8}$ → **10a**	−2.2		−0.6		1.2	
7 + $\mathbf{C_8}$ → **10b**	−5.6		−4.7		−3.6	
10a → **ts8a**		9.1		6.5		4.1
10b → **ts8b**		16.5		15.1		13.7
10a → **5** + $\mathbf{C_2}$	−3.0		−4.9		−7.4	
10b → **7** + $\mathbf{C_8}$	5.6		4.7		3.6	

[a] Total electronic energy difference + ZPE correction (kcal/mol) calculated at B3LYP/LANL2DZ level. [b] Activation energy including ZPE correction (kcal/mol) calculated at B3LYP/LANL2DZ level.

kcal/mol by cyclohexane, respectively. Since these changes are parallel to the decreases in activation energies of **ts4b**, **ts4a**, and **ts8b**, solvation does not change the competitiveness of the reactions involving these transition states. As an exception, in the metathesis of tungsten heptylidene, **5** (see Figure 3), solvation by chloroform increases the activation energy of **ts5a** by 3.0 kcal/mol and at the same time decreases the activation energy of **ts5b** by 0.3 kcal/mol making the formation of the metallocyclobutane intermediate, **9b**, more favorable than **9a**. When the effects of solvation on the overall metathetic cycle is considered, solvation by chloroform affects to favor formation of ethylene, C_2, and heptylidene, **5**, by 1.0 kcal/mol, and cyclohexane shows no significant effect.

4. Conclusions

Since atomic carbon is highly energetic, formation of **3b** is an exothermic process and with this excess energy, catalytic metathesis reactions take place easily at room temperature.[47]

In this study, both electronic and thermal energies are taken into consideration, and it is seen that there is a coincidence between the calculated values. In both cases, formation of heptylidene is more favorable than formation of methylidene. This result is in agreement with the results from the quantum-mechanical calculations employed by Jordaan et al. for 1-octene metathesis with Grubbs 1 catalyst, indicating formation of the heptylidene was kinetically and thermodynamically more favorable than the formation of the methylidene;[25] however, since the free-energy difference between the highest energy structures of the two paths, **ts3a** and **ts4b**, is 4.3 kcal/mol (see Figure 2), these two paths are competitive, and both alkylidene species may form. Similarly, in the formation of 7-tetradecene, C_{14}, degenerative path is more favorable than productive path by 4.7 kcal/mol between **ts6a** and **ts6b** (Figure 3), while in the formation of ethylene, C_2, productive path is favorable by 3.2 kcal/mol between **ts7a** and **ts7b** (Figure 4). However, in both cases, degenerative and productive paths are competitive, and solvation does not have any significant effect on these steps.

When the two productive steps are compared, in the formation of 7-tetradecene, C_{14}, the largest free-energy of activation ($\Delta G^{\ddagger}_{298}$ = 24.3 kcal/mol Figure 3, Table 3) is associated with formation of the metallocyclobutane species **9a**; however, transition state **ts6a** is clearly the highest point on the calculated free-energy profile, and its formation is thus rate-determining. On the other hand, in the formation of ethylene, formation of the metallocyclobutane **10a** is the rate-determining step since **ts7a** is the highest energy structure on the surface. Solvation by chloroform decreases the activation energy of **ts6a** by 2.6 kcal/mol, where it increases the activation energy of **ts7a** by 0.8 kcal/mol.

Acknowledgment. This research was supported by the TUBITAK (Scientific and Technical Research Council of the Turkish Republic) under Grant 104T402.

Supporting Information Available: Z-matrix data, Mulliken charge distributions and energy values of the optimized structures. This material is available free of charge via the Internet at http://pubs.acs.org.

References and Notes

(1) Ivin, K. J.; Mol, C. J. *Olefin Metathesis and Metathesis Polymerization*; Accademic Press: San Diego, 1997.
(2) Grubbs, R. H. *Handbook of Olefin Metathesis*; Wiley-VCH: Weinheim, Germany, 2003.
(3) Trnka, T. M.; Grubbs, R. H. *Acc. Chem. Res.* **2001**, *34*, 18.
(4) Astruc, D. *New J. Chem.* **2005**, *29*, 42.
(5) Schrock, R. R. *J. Organomet. Chem.* **1986**, *300*, 249.
(6) Hérisson, J. L.; Chauvin, Y. *Macromol. Chem.* **1971**, *141*, 161.
(7) Adlhart, C.; Chen, P. *J. Am. Chem. Soc.* **2004**, *126*, 3496.
(8) Sanford, M. S.; Ulman, M.; Grubbs, R. H. *J. Am. Chem. Soc.* **2001**, *123*, 749.
(9) Sanford, M. S.; Love, J. A.; Grubbs, R. H. *J. Am. Chem. Soc.* **2001**, *123*, 6543.
(10) Ulman, M.; Grubbs, R. H. *Organometallics* **1998**, *17*, 2484.
(11) Love, J. A.; Sanford, M. S.; Day, M. W.; H, G. R. *J. Am. Chem. Soc.* **2003**, *125*, 10103.
(12) Hinderling, C.; Adlhart, C.; Chen, P. *Angew. Chem., Int. Ed.* **1998**, *37*, 2685.
(13) Adlhart, C.; Hinderling, C.; Baumann, H.; Chen, P. *J. Am. Chem. Soc.* **2000**, *122*, 8204.
(14) Adlhart, C.; Chen, P. *Helv. Chim. Acta* **2003**, *86*, 941.
(15) Adlhart, C.; Chen, P. *Helv. Chim. Acta* **2000**, *83*, 2192.
(16) Adlhart, C.; Volland, M. A. O.; Hofmann, P.; Chen, P. *Helv. Chim. Acta* **2000**, *83*, 3306.
(17) Volland, M. A. O.; Hansen, S. M.; Hofmann, P. In *Chemistry at the Beginning of the Third Millennium: Molecular Design, Supramolecules, Nanotechnology and Beyond*; Fabrizzi, L., Poggi, A. , Eds.; Springer: Berlin, 2000.
(18) Basu, K.; Cabral, J. A.; Paquette, L. A. *Tetrahedron Lett.* **2002**, *43*, 5453.
(19) Dias, E. L.; Nguyen, S. T.; Grubbs, R. H. *J. Am. Chem. Soc.* **1997**, *119*, 3887.
(20) Hansen, S. M.; Rominger, F.; Metz, M.; Hofmann, P. *Chem.—Eur. J.* **1999**, *5*, 557.
(21) Bernardi, F.; Bottoni, A.; Miscione, G. P. *Organometallics* **2003**, *22*, 940.
(22) Vyboishchikov, S. F.; Bühl, M.; Thiel, W. *Chem.—Eur. J.* **2002**, *8*, 3962.
(23) Aagaard, O. M.; Meier, R. J.; Buda, F. *J. Am. Chem. Soc.* **1998**, *120*, 7174.
(24) Meier, R. J.; Aagaard, O. M.; Buda, F. *J. Mol. Catal. A* **2000**, *160*, 189.
(25) Jordaan, M.; van Helden, P.; van Sittert, C. G. C. E.; Vosloo, H. C. M. *J. Mol. Catal. A* **2006**, *254*, 145.
(26) Riley, K. E.; Merz, K. M., Jr *J. Phys. Chem. A* **2007**, *111*, 6044.
(27) Shuqiang, N.; Hall, M. B. *Chem. Rev.* **2000**, *100*, 353.
(28) Buda, C.; Cundari, T. R. *J. Mol. Struct.* **2004**, *686*, 137.
(29) Burdett, K. A.; Haris; L. D.; Margl, P.; Mokhtar-Zadeh, T.; Saucier, P. C.; Wasserman, E. P. *Organometallics* **2004**, *124*, 2027.
(30) Fomine, S.; Martinez Vargas, S.; Tlenkopatchev, M. A. *Organometallics* **2003**, *22*, 93.
(31) Cavallo, L. *J. Am. Chem. Soc.* **2002**, *124*, 8965.
(32) Adlhart, C.; Chen, P. *Angew. Chem., Int. Ed.* **2002**, *41*, 4484.
(33) Fomine, S.; Ortega, J. V.; Tlenkopatchev, M. A. *Organometallics* **2005**, *24*, 5696.
(34) Fomine, S.; Ortega, J. V.; Tlenkopatchev, M. A. *J. Mol. Catal. A* **2005**, *236*, 156.
(35) Tlenkopatchev, M. A.; Fomine, S. *J. Organomet. Chem.* **2001**, *630*, 157.
(36) Fomine, S.; Vargas Ortega, J.; Tlenkopatchev, M. A. *J. Organomet. Chem.* **2006**, *691*, 3343.
(37) Fomine, S.; Ortega, J. V.; Tlenkopatchev, M. A. *J. Mol. Catal. A* **2007**, *263*, 121.
(38) Spivak, G. J.; Coalter, J. N., III *Organometallics* **1998**, *17*, 999.
(39) Handzlik, J. *Surf. Sci.* **2007**, *601*, 2054.
(40) Handzlik, J. *J. Phys. Chem. C* **2007**, *111*, 9337.
(41) Buchmeiser, M. R.; Wang, D.; Naumov, S.; Wurst, K. *J. Organomet. Chem.* **2006**, *691*, 5391.
(42) Poater, A.; Solans-Monfort, X.; Clot, E.; Copéret, C.; Eisenstein, O. *J. Am. Chem. Soc.* **2007**, *129*, 8207.
(43) van Rensburg, W. J.; Steynberg, P. J.; Kirk, M. M.; Meyer, W. H.; Forman, G. S. *J. Organomet. Chem.* **2006**, *691*, 5312.
(44) Forman, G. S.; McConnell, A. E.; Tooze, R. P.; van Rensburg, W. J.; Meyer, W. H.; Kirk, M. M.; Dwyer, C. L.; Serfontein, D. W. *Organometallics* **2005**, *24*, 4528.
(45) Frenking, G.; Solà, M.; Vyboishchikov, S. F. *J. Organomet. Chem.* **2005**, *690*, 6178.
(46) Vyboishchikov, S. F.; Thiel, W. *Chem.—Eur. J.* **2005**, *11*, 3921.
(47) Düz, B.; Yüksel, D.; Ece, A.; Sevin, F. *Tetrahedron Lett.* **2006**, *47*, 5167.
(48) Gill, P. M. W.; Johnson, B. G.; Pople, J. A.; Frisch, M. J. *Chem. Phys. Lett.* **1992**, *197*, 499.
(49) Pople, J. A.; Gill, P. M. W.; Johnson, B. G. *Chem. Phys. Lett.* **1992**, *199*, 557.
(50) Kohn, W.; Sham, L. J. *Phys. Rev.* **1965**, *140*, A1133.
(51) Parr, R. G.; Yang, W. *Density-functional Theory of Atoms and Molecules*; Oxford University Press: Oxford, 1989.
(52) Becke, A. D. *J. Chem. Phys.* **1992**, *97*, 9173.

(53) Frisch, M. J.; Trucks, G. W.; Schlegel, H. B.; Scuseria, G. E.; Robb, M. A.; Cheeseman, J. R.; Montgomery, J. A., Jr.; Vreven, T.; Kudin, K. N.; Burant, J. C.; Millam, J. M.; Iyengar, S. S.; Tomasi, J.; Barone, V.; Mennucci, B.; Cossi, M.; Scalmani, G.; Rega, N.; Petersson, G. A.; Nakatsuji, H.; Hada, M.; Ehara, M.; Toyota, K.; Fukuda, R.; Hasegawa, J.; Ishida, M.; Nakajima, T.; Honda, Y.; Kitao, O.; Nakai, H.; Klene, M.; Li, X.; Knox, J. E.; Hratchian, H. P.; Cross, J. B.; Adamo, C.; Jaramillo, J.; Gomperts, R.; Stratmann, R. E.; Yazyev, O.; Austin, A. J.; Cammi, R.; Pomelli, C.; Ochterski, J. W.; Ayala, P. Y.; Morokuma, K.; Voth, G. A.; Salvador; P.; Dannenberg, J. J.; Zakrzewski, V. G.; Dapprich, S.; Daniels, A. D.; Strain, M. C.; Farkas, O.; Malick, D. K.; Rabuck, A. D.; Raghavachari, K.; Foresman, J. B.; Ortiz, J. V.; Cui, Q.; Baboul, A. G.; Clifford, S.; Cioslowski, J.; Stefanov, B. B.; Liu, G.; Liashenko, A.; Piskorz, P.; Komaromi, I.; Martin, R. L.; Fox, D. J.; Keith, T.; Al-Laham, M. A.; Peng, C. Y.; Nanayakkara, A.; Challacombe, M.; Gill, P. M. W.; Johnson, B.; Chen, W.; Wong, M. W.; Gonzales, C.; Pople, J. A. *Gaussian 03, revision B.03*; Gaussian, Inc.: Pittsburgh, PA, 2003.

(54) Becke, A. D. *J. Chem. Phys.* **1993**, *98*, 5648.

(55) Lee, C.; Yang, W.; Parr, R. G. *Phys. Rev.* **1998**, *B 37*, 785.

(56) Hay, P. J.; Wadt, W. R. *J. Chem. Phys.* **1985**, *82*, 270.

(57) Check, C. E.; Faust, T. O.; Bailey, J. M.; Wright, J.; Gilbert, T. M.; Sunderlin, L. S. *J. Phys. Chem. A* **2001**, *105*, 8111.

(58) Mulliken, R. S. *J. Chem. Phys.* **1955**, *23*, 1833.

(59) Foresman, J. B.; Keith, T. A.; Wiberg, K. B.; Snoonian, J.; Frisch, M. J. *J. Phys. Chem.* **1996**, *100*, 16098.

(60) Cundari, T. R.; Gordon, M. S. *Organometallics* **1992**, *11*, 55.

(61) Cho, H-G.; Andrews, L. *Organometallics* **2005**, *24*, 5678.

JP076044C